

Supporting Information for:

One-Pot route to produce the porous assemblies by the PISA of
star architecture copolymers: A simulation study

Junfeng Wang¹, Jiawei Li¹, Qiang Yao¹, Xiaoli Sun¹, Youguo Yan¹, and Jun Zhang^{1,*}

¹College of Science, China University of Petroleum (East China), Qingdao, Shandong
266580, People's Republic of China

*Corresponding Authors, Email: zhangjun.upc@gmail.com (J. Zhang).

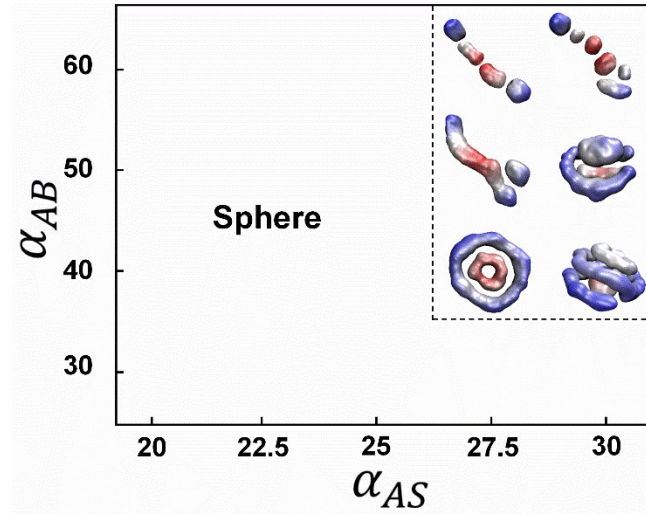


Fig. S1. The morphology phase diagram formed by the PISA of A_3B_{12} linear copolymers at $\alpha_{BS} = 60$ in terms of different repulsion interaction parameters α_{AS} and α_{AB} .

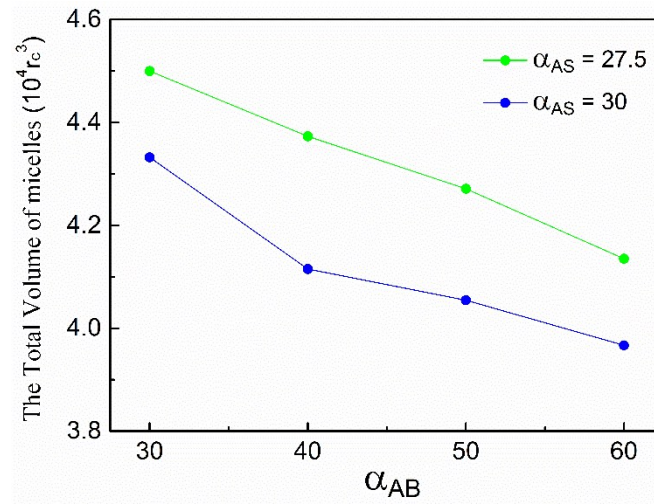


Fig. S2. The total volume of micelles formed by the PISA of $A_3(B_6)_2$ at different α_{AS} and α_{AB} .

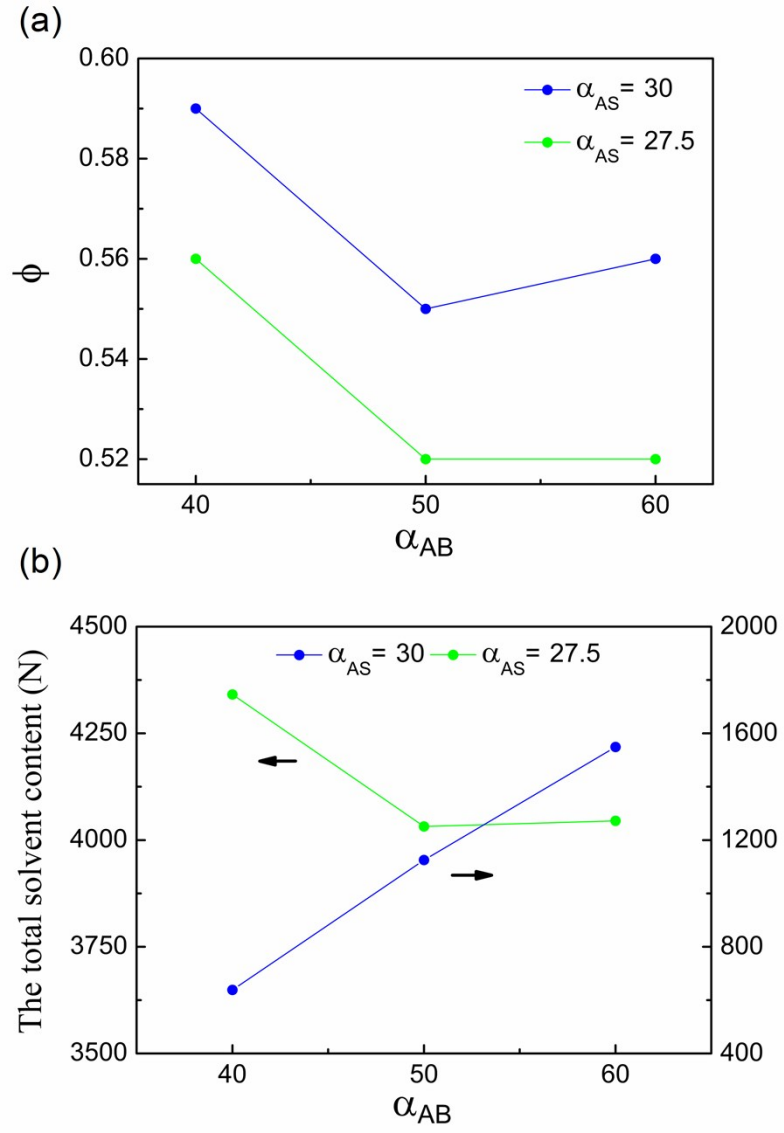


Fig. S3. (a) The number of the solvophilic blocks in the micelles (ϕ) with different α_{AS} and α_{AB} . (b) The total solvent content with different α_{AS} and α_{AB} .

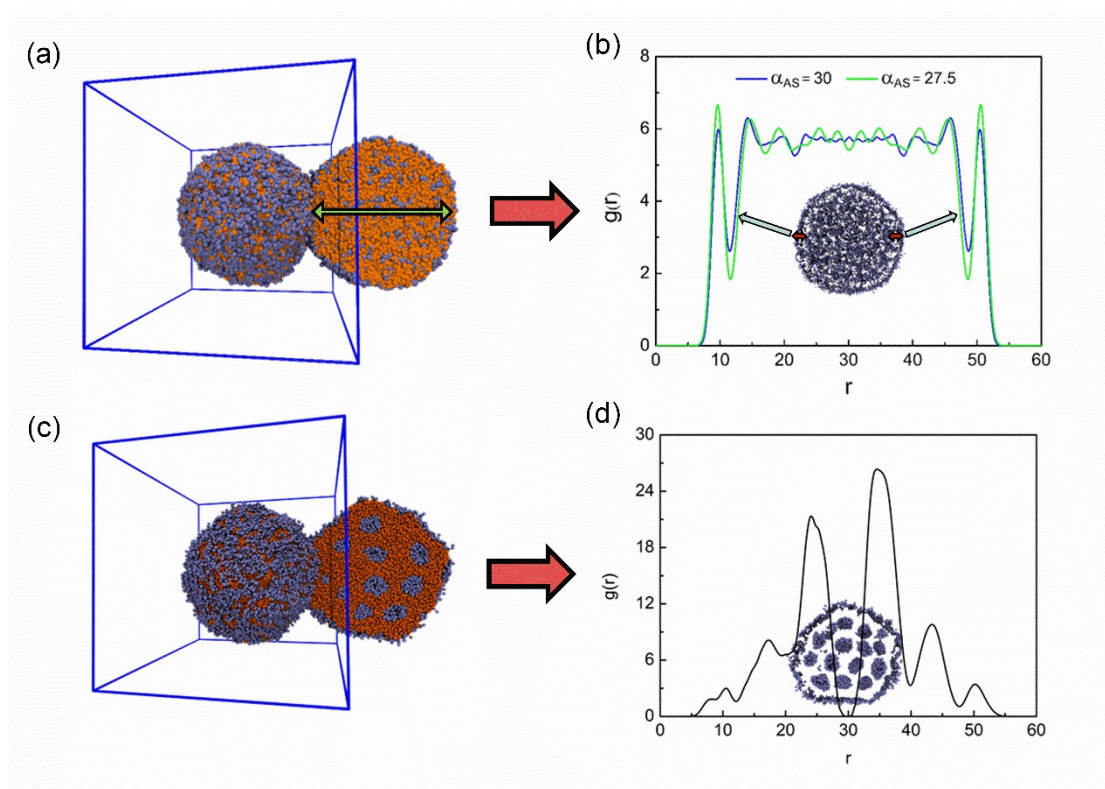


Fig. S4. (a) The self-assembly morphology and its section of star architecture copolymers at $\alpha_{AB} = 30$. (b) The radial distribution function of solvophilic blocks at $\alpha_{AS} = 30$ and 27.5 , $\alpha_{AB} = 30$. (c) The self-assembly morphology and its section of the porous vesicle at $\alpha_{AS} = 30$, $\alpha_{AB} = 60$. (d) The radial distribution function of solvophilic blocks.

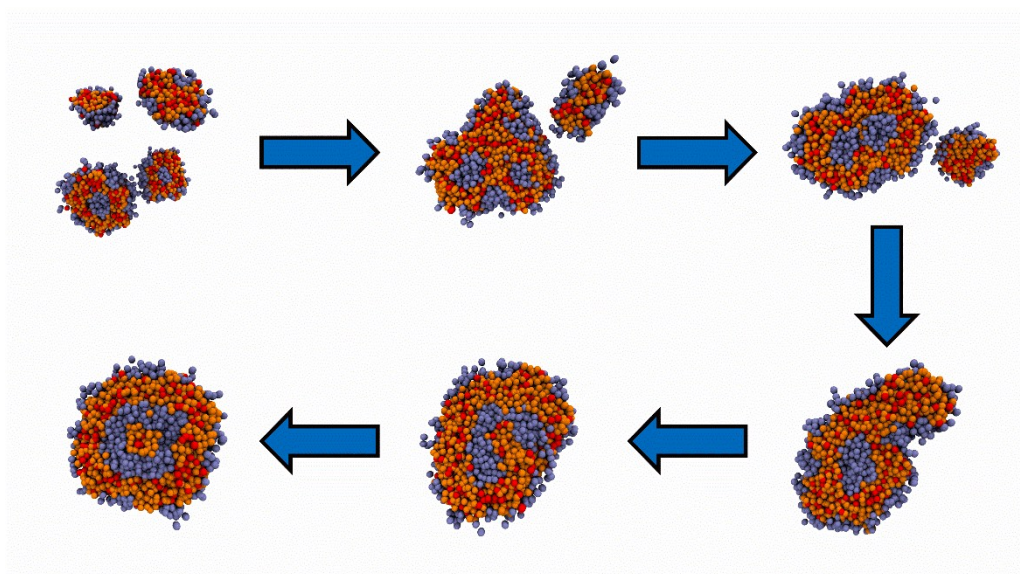


Fig. S5. The self-assembly progress of the vesicle with a ring-like cavity.

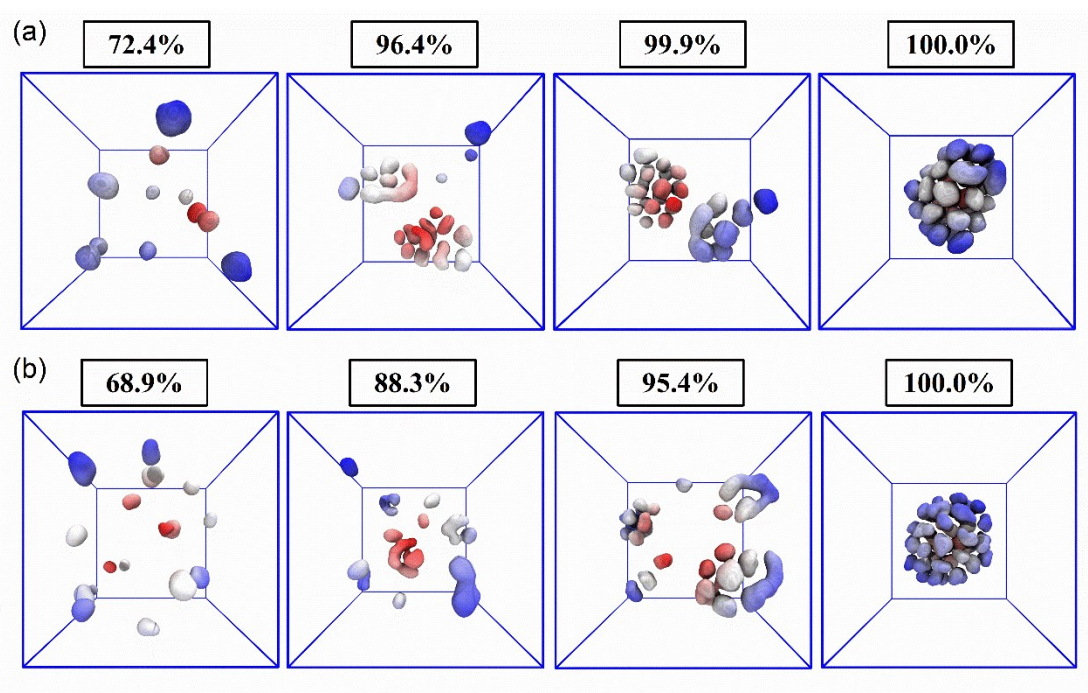


Fig. S6. (a) The PISA progress of $A_3(B_6)_2$ star architecture copolymers at $\alpha_{AS} = 27.5$ and $\alpha_{AB} = 50$ with the conversion of monomers increasing. (a) The PISA progress of $A_3(B_6)_2$ star architecture copolymers at $\alpha_{AS} = 27.5$ and $\alpha_{AB} = 40$ with the conversion of monomers increasing.

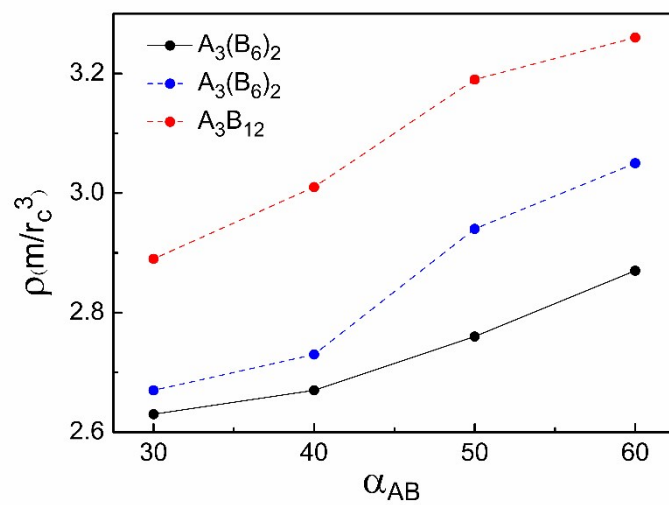


Fig. S7. The density of solvophobic blocks in the porous micelles with various α_{AB} at $\alpha_{AS} = 30$ (dashed line), and the density of solvophobic blocks with angle restricted with various α_{AB} at $\alpha_{AS} = 30$ (solid line).

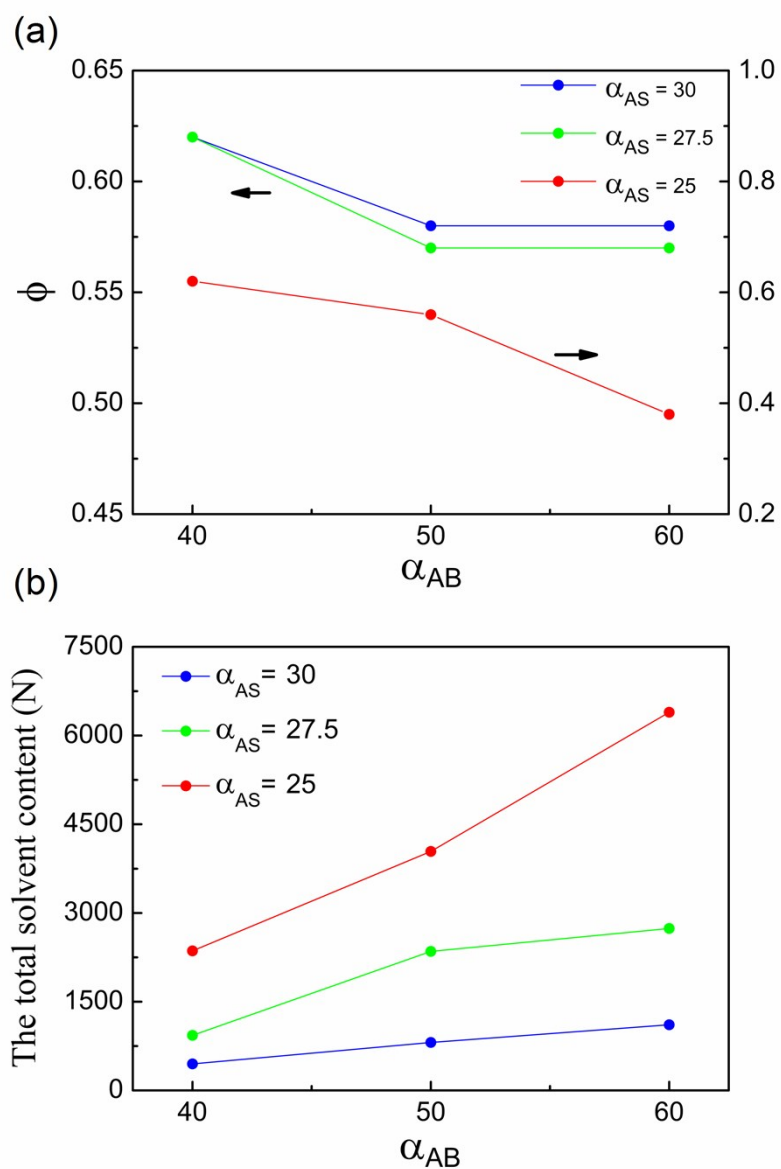


Fig. S8. When the angle among the beads closest to the center of star architecture is restricted, (a) The number of the solvophilic blocks in the micelles with different α_{AS} and α_{AB} . (b) The solvent possession per solvophilic block in the micelles with different α_{AS} and α_{AB} . (c) The total solvent content with different α_{AS} and α_{AB} .

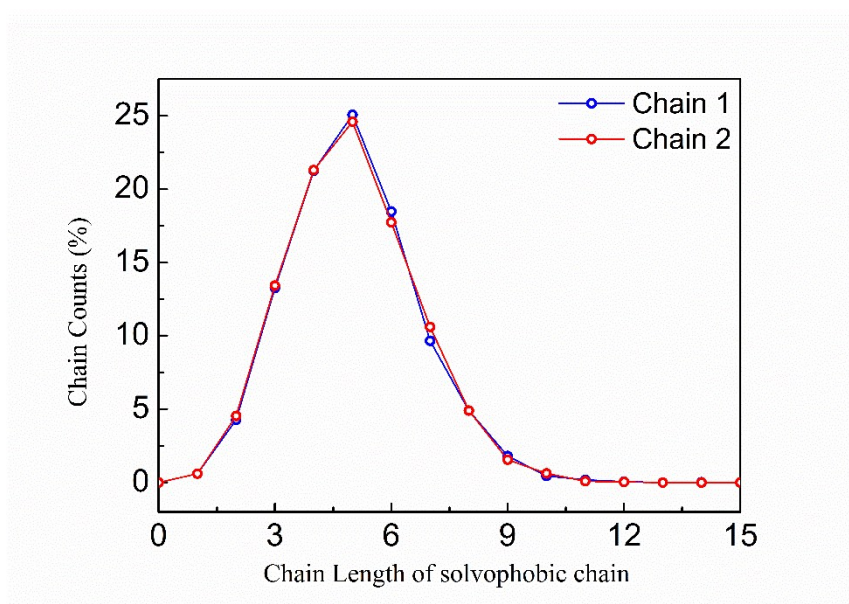


Fig. S9. The chain length distribution of two solvophobic chains of star architecture copolymer (Take the condition of $\alpha_{AS} = 30$, $\alpha_{AB} = 60$ as the example).

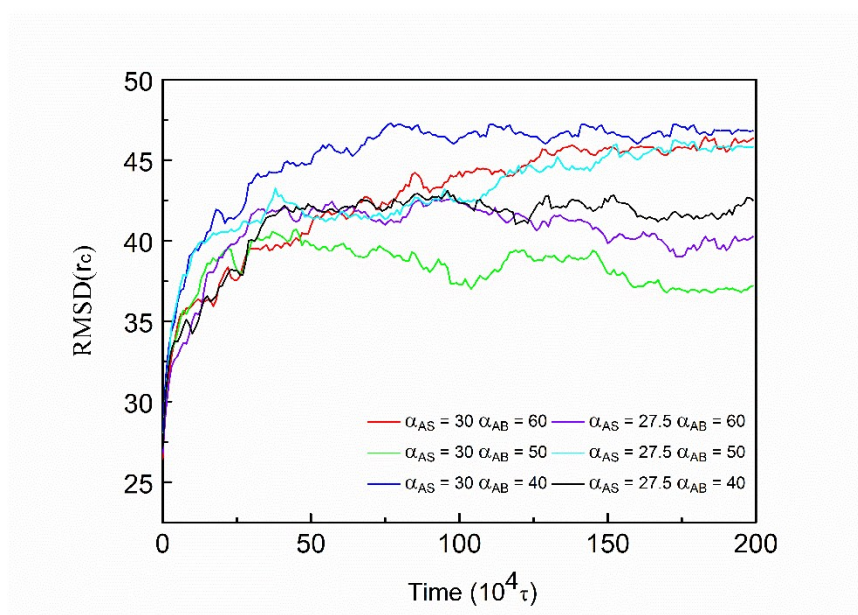


Fig. S10. The root-mean-square deviation (RMSD) of star architecture copolymers over time at various α_{AS} and α_{AB} .

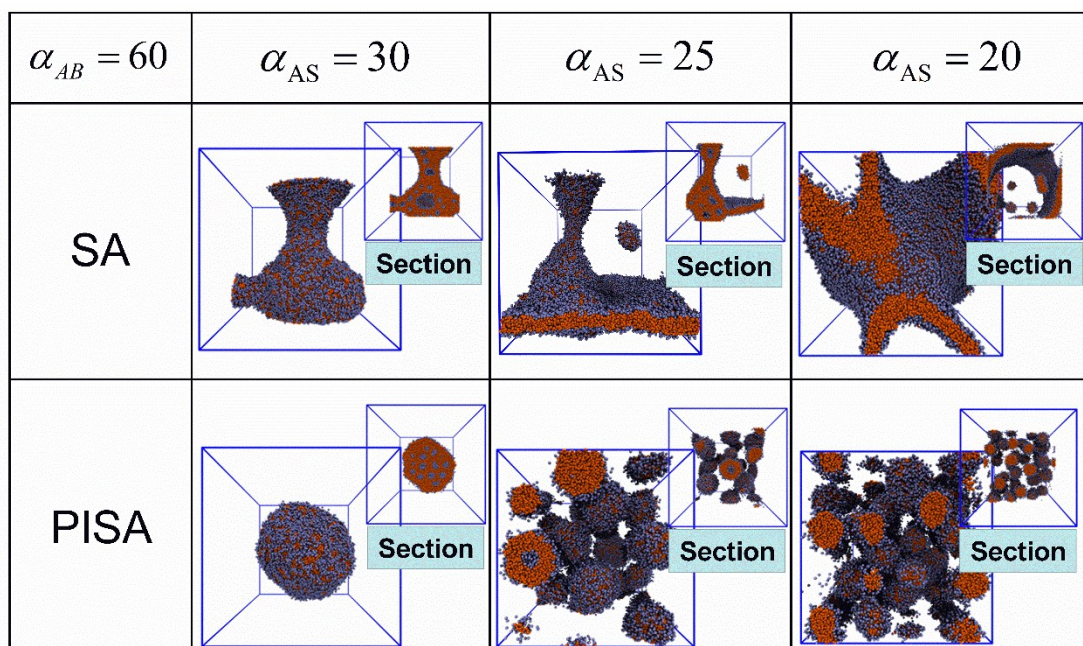


Fig. S11. The morphologies obtained by PISA and self-assembly of amphiphilic copolymers with the same chain length distribution at various α_{AS} and α_{AB} .

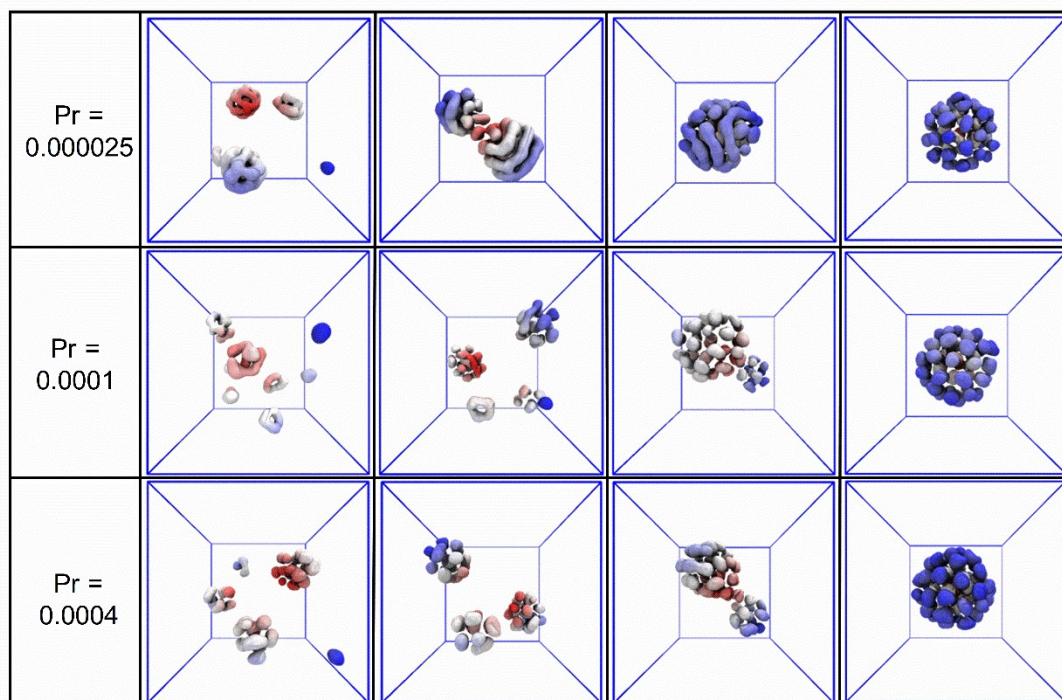


Fig. S12. The self-assembly progress of PISA at different polymerization rate (P_r).